Selective hydrogenolysis of glycerol to propanediols on supported Cu-containing bimetallic catalysts

Jinxia Zhou,[a] Liyuan Guo,[a] Xinwen Guo,[b] Jingbo Mao[a] and Shuguang Zhang*[a,b]

Received 28th April 2010, Accepted 20th July 2010
DOI: 10.1039/c0gc00058b

Supported Cu-containing bimetallic catalysts were prepared and used to convert glycerol to propanediols. The effects of supports, metals, metal loadings, and impregnation sequences were examined. A synergistic effect was observed between Cu and Ag when they were impregnated on γ-Al_2O_3. Characterizations revealed that the addition of Ag not only resulted in an *in situ* reduction of CuO, but also improved the dispersion of the Cu species on the support. A Cu–Ag/Al_2O_3 catalyst with optimal amounts of Cu and Ag (Cu/Ag molar ratio 7 : 3, 2.7 mmol Cu+Ag per gram of γ-Al_2O_3) showed a near 100% selectivity to propanediols with a glycerol conversion of about 27% under mild reaction conditions (200 °C, 1.5 MPa initial H_2 pressure, 10 h, (Cu+Ag)/glycerol molar ratio of 3/100). Compared with a commercial copper chromite catalyst commonly used for this reaction, the Cu–Ag/Al_2O_3 catalyst had much higher activity and did not need a reduction pretreatment.

1. Introduction

As important commodity chemicals, propanediols are widely used as functional fluids such as de-icing reagents, antifreeze/coolants, and as precursors for the syntheses of unsaturated polyester resins and pharmaceuticals.[1] Propanediols are currently produced from propylene *via* a process involving selective propylene oxidation to propylene oxide and subsequent hydrolysis.[2,3] The process is restricted by the supply of propylene derived from crude oil, and that stimulated a search for more economical and renewable alternative feeds. Glycerol is a renewable chemical which is usually produced by steam splitting or saponification of animal fat or vegetable oil. Now it can also be obtained as a major by-product from the biodiesel production process.[4] Readily available glycerol has made the catalytic hydrogenolysis of glycerol to propanediols a highly viable alternative route. The reactions and processes for glycerol conversion to valuable compounds have been well covered in previous reviews.[5,6] The following discussion intends to provide more details about catalyst preparation and testing conditions for glycerol hydrogenolysis.

Supported noble metals and transition metal oxides have been reported in the literature as catalysts for the hydrogenolysis of glycerol. Noble metal based catalysts are usually more active than transition metal oxide catalysts, but the selectivity to propanediols is lower.[3] Among several supported metal catalysts (metal: Rh, Ru, Pt, Pd; support: active carbon, SiO_2, Al_2O_3), Furikado *et al.*[7] found that Rh/SiO_2 was the most active and selective one, with a glycerol conversion of 19.6% and a propanediol selectivity of 39.8% at 120 °C, 8 MPa initial H_2 pressure, and 10 h. Feng *et al.*[8] found that a TiO_2 supported Ru catalyst exhibited a markedly high activity, 90.1% glycerol conversion at 180 °C and 5 MPa H_2 pressure, but that the propanediol selectivity was only 20.6%. The use of supported noble metal catalysts with various acidic materials was also studied.[9–12] The combination of a Ru/C and an Amberlyst resin presented a glycerol conversion of 79.3% and a propanediol selectivity of 74.7% at 120 °C, 8 MPa initial H_2 pressure, and 10 h.[9] The use of Ru/C with other acidic materials, such as niobia, 12-tungstophosphoric acid (TPA) supported on zirconia, the caesium salt of TPA and the caesium salt of TPA supported on zirconia, was studied by Balaraju *et al.*[11] They found a linear correlation between conversion and acidity on the catalysts. Alhanash *et al.*[12] prepared a bifunctional catalyst by loading Ru onto a heteropoly acid salt $Cs_{2.5}H_{0.5}[PW_{12}O_{40}]$, which achieved 96% selectivity to 1,2-propanediol at 21% glycerol conversion at 150 °C and 5 MPa initial H_2 pressure in 10 h. As of supported bimetallic noble metal catalysts, Ma *et al.*[13] discovered a promoting effect of Re on the catalytic performances of Ru/Al_2O_3, Ru/C, and Ru/ZrO_2, both on the conversion of glycerol and the selectivity to propanediols.

Transition metal oxide catalysts used for the hydrogenolysis of glycerol often exhibit good selectivity towards propanediols. Chaminand *et al.*[3] showed that nearly 100% selectivity to 1,2-propanediol was achieved on a CuO/ZnO catalyst, but the activity of the catalyst was so low that it took 90 h to reach 19% glycerol conversion. Wang and Liu[14] obtained a selectivity of 83.6% to 1,2-propanediol at 22.5% glycerol conversion at 200 °C and 4.2 MPa initial H_2 pressure, after 12 h on a Cu–ZnO catalyst (Cu/glycerol = 3 wt%). Dasari *et al.*[15] reported that a commercial copper chromite catalyst (pre-reduced at 300 °C) converted glycerol to 1,2-propanediol with a selectivity of 85.0% at 54.8% conversion at 200 °C and 1.4 MPa initial H_2 pressure, after 24 h. Considering the good performance of copper chromite catalysts under relatively mild reaction conditions as well as the vulnerability of noble metal catalysts to impurities in glycerol, the process using copper chromite is considered to be the most promising one for commercialization.[4,15] Another catalyst that

[a]*College of Environmental and Chemical Engineering, Dalian University, Dalian, 116622, China. E-mail: dluzhang@126.com; Fax: +86-411-87402449; Tel: +86-411-87403214*
[b]*State Key Laboratory of Fine Chemicals, Dalian University of Technology, Dalian, 116012, China*

may be used at relatively low hydrogen pressure[16] or even without hydrogen[17] is RANEY® Ni.

In spite of many research efforts, this important reaction has not been successfully commercialized due to several common drawbacks with the catalysts used. The main problem of supported noble metal catalysts is the low selectivity towards propanediols. The Cu-based catalysts exhibited superior performances in terms of the selectivity towards propanediols, but their activities are usually low. The Cu on these catalysts is initially in an oxidic state. In order to achieve a decent activity, the catalysts often need to be reduced *in situ* under reaction conditions with very high H_2 pressure,[14] or to be pre-reduced to generate Cu species which are catalytically active under mild reaction conditions.[18]

In previous work,[19] we reported that a selectivity to propanediols of about 97% with a glycerol conversion of about 50% was achieved on a Cu/Al_2O_3 catalyst. Like most transition metal catalysts, however, this Cu/Al_2O_3 catalyst had to be pre-reduced in H_2. By employing another metal besides Cu to prepare supported bimetallic catalysts, the present study aimed at eliminating the pre-reduction step while maintaining or further improving the activity and selectivity. Various characterization techniques were applied to investigate the *in situ* generation of active sites under reaction conditions.

2. Experimental

2.1 Catalyst preparation

Our Cu-based catalysts were synthesized using an incipient wetness impregnation method similar to those described in the literature[20,21] with aqueous solutions of $Cu(NO_3)_2{\cdot}3H_2O$ and/or another metal nitrate ($AgNO_3$, $Zn(NO_3)_2{\cdot}6H_2O$, $Cr_2(NO_3)_3{\cdot}3H_2O$, $Ni(NO_3)_2{\cdot}3H_2O$, or $Co(NO_3)_3{\cdot}H_2O$). The supports used in this study include γ-Al_2O_3 (Shandong Filiale of China Aluminium Co., Ltd., China), HY zeolite (Wenzhou Huahua Co., Ltd., China), HZSM-5 zeolite (Nankai University Catalyst Co., Ltd., China), and Hβ zeolite (PQ Zeolites B.V.). Some physical properties of these supports are summarized in Table 1.

After impregnation, the catalysts were dried at 110 °C for 12 h and calcined in air for 3 h at 400 °C, except in the study of calcination temperature. Unless specifically stated, these catalysts were tested or characterized directly after the calcination without a pre-treatment in H_2. In a few cases, the catalysts were pre-reduced at 300 °C for 3 h in a H_2 stream (30 ml min^{-1}), and then the names were postfixed with (H_2), for example, $Cu/Al_2O_3(2.0)(H_2)$. All catalysts were in powder form with particle size less than 0.32 mm in diameter. The catalysts prepared were designated as CuX/Support(S)(Cu:X), in which X represents any other metal that was loaded besides Cu, S represents the amount of total metals (mmol) loaded on a support (per gram), and Cu:X is the molar ratio of Cu to the other metal. For example, $CuAg/Al_2O_3(2.7)(7:3)$ is a catalyst with 2.7 mmol Cu plus Ag, a Cu/Ag molar ratio 7 : 3, supported on 1 g of Al_2O_3.

A copper chromite catalyst (Engelhard Corporation, US) was tested for comparison purposes.

Table 1 Physical properties of supports

Support	SiO_2/Al_2O_3 (mol/mol)	BET surface area/$m^2\ g^{-1}$	Pore volume/ mL g^{-1}
γ- Al_2O_3		313	0.37
HY	5.6	718	0.42
HZSM-5	48	356	0.31
Hβ	27	731	0.87

2.2 Catalyst characterization

X-Ray Diffraction (XRD) patterns of the catalysts were recorded at room temperature on an X-ray diffractometer (D/max-2400) with a graphite monochromator attachment, utilizing Ni-filtered Cu-Kα radiation (40 kV, 100 mA) with a scanning speed (2θ) of 1° per min.

Nitrogen adsorption experiments for pore size distribution, pore volume, and surface area measurements were conducted on an AUTOSORB-1 instrument (Quantachrome). All samples were calcined at 350 °C under vacuum before the measurements.

Temperature Programmed Reduction (TPR) studies of the catalysts were carried out in a 10% H_2/Ar gas mixture at a flow rate of 50 ml min^{-1} with a temperature ramp of 10 °C min^{-1}. Before TPR tests the catalysts were pretreated in argon at 300 °C for 2 h. Hydrogen consumption was monitored using a thermal conductivity detector (TCD).

X-Ray Photoelectron Spectroscopy (XPS) measurements were performed on an ESCALAB-250 spectrometer with a monochromatic X-ray source (Al Kα line of 1486.6 eV energy and 150 W) to characterize surface species on the catalysts. XPS elemental spectra were acquired in a fixed analyzer transmission mode with steps of 0.1 eV energy at a pass energy of 50 eV. All spectra were aligned based on the adventitious C 1 s peak at 284.6 eV. The spectra were fitted with an XPSPEAK 41 program using a Shirley background and Gaussian line shapes for the deconvolution into individual states and for obtaining peak areas.

2.3 Catalytic activity measurement

The hydrogenolysis of glycerol was carried out in a high throughput batch reactor system consisting of ten independent stainless steel autoclaves (165 ml each) with mechanical stirring. An aqueous solution of glycerol (50 wt% concentration) prepared with pure glycerol (>99%, China National Medicines Corporation Ltd., China) and deionized water was used as feed. In a typical run, 65 g of the glycerol solution and a specified quantity of the catalyst were loaded into the reactor. The molar ratio of the active metal(s) on the catalyst to the glycerol (M:G) was 3 : 100. The reactor was purged five times with H_2 (99.99%; Dalian F.T.Z Gredit Chemical Technology Development Co., Ltd.) and pressurized with H_2 to 1.5 MPa at room temperature. With stirring at 400 RPM, the mixture of the glycerol and the catalyst was heated to 200 °C and maintained for 10 h. The stirring speed was selected to eliminate the influence of external mass transfer and to avoid creating splash inside the reactor which would make sampling and temperature control very difficult. Hydrogen was fed on demand so as to keep the total reaction pressure at 3.6 MPa during the 10 h period.

After the reaction, the gas phase products were collected in a gas bag and the liquid phase products were separated from the

catalyst by filtration. These products were analyzed using a gas chromatograph (GC HP5890) equipped with a flame ionization detector. The GC column used was a PEG2W capillary column (30 m × 0.32 mm × 0.5 μm) manufactured by Dalian Institute of Chemical Physics, Chinese Academy of Sciences. Solutions of *n*-butanol with known amounts of internal standards were prepared and used for quantification of various glycerol-derived compounds in the products.

The conversion of glycerol, the selectivity, and the yield of propanediols were used to evaluate the performance of each catalyst. They were defined by the following equations. The amount of glycerol converted was calculated from the total amount of carbon based species formed in the product. Only trace amount of product was detected in the gas phase. The carbon on a used catalyst was analyzed with thermogravimetry and C/H elemental analyses (results not shown here). Overall carbon balance in the product was >98%. Products besides propanediols, such as ethylene glycol and 1-propanol, were also identified and listed as "Others" in the tables below. Repeated runs showed that data variation was in the range of ±5% (relative value).

$$\text{Conversion (\%)} = \frac{\text{amount of glycerol converted (mole)}}{\text{total amount of glycerol in the feed (mole)}} \times 100$$

$$\text{Selectivity (\%)} = \frac{\text{amount of glycerol converted to a product (mole)}}{\text{amount of glycerol converted (mole)}} \times 100$$

$$\text{Yield (\%)} = [\text{Conversion (\%)} \times \text{Selectivity (\%)}]/100$$

3. Results and discussion

3.1 Investigation of catalyst composition

Active metal selection. A series of γ-Al_2O_3 supported bimetallic catalysts were prepared and tested without pre-reduction treatment. One of the two metals was Cu, and the other one was selected from Ag, Zn, Cr, Ni, or Co. Two supported monometallic catalysts, Cu/Al_2O_3(1.9) and Ag/Al_2O_3(0.8), were also prepared. These two catalysts and their physical mixture were tested for comparison with the $CuAg/Al_2O_3$(2.7)(7 : 3) catalyst. The reaction results are shown in Table 2.

The Cu-containing catalysts presented pretty high selectivity to propanediols. This is in agreement with the literature, which shows that copper-based catalysts are usually selective towards the formation of propanediols with little or no selectivity towards ethylene glycol and other degradation by-products.[3,14,15,19] On all these catalysts, the majority of the propanediols formed was 1,2-propanediol (1,2-PD) and the amount of 1,3-propanediol (1,3-PD) was very small. However, the activities of these catalysts differed significantly. $CuAg/Al_2O_3$ was most active, with a glycerol conversion of 27%, 3–6 times that of the $CuZn/Al_2O_3$ and $CuCr/Al_2O_3$ catalysts. Other bimetallic catalysts tested, $CuNi/Al_2O_3$ and $CuCo/Al_2O_3$ (results not shown here), also showed poor activities.

Table 2 Hydrogenolysis of glycerol on Al_2O_3 supported bimetallic catalysts

Catalyst	M : G	Conv. (%)	Selectivity (%)		
			1,2-PD	1,3-PD	Others
$CuAg/Al_2O_3$(2.7)(7 : 3)	3 : 100	27	96	0	4
$CuZn/Al_2O_3$(2.7)(7 : 3)	3 : 100	6	94	0	6
$CuCr/Al_2O_3$(2.7)(7 : 3)	3 : 100	1	92	2	6
Cu/Al_2O_3(1.9)	2.1 : 100	2	83	0	17
Ag/Al_2O_3(0.8)	0.9 : 100	8	94	0	6
Cu/Al_2O_3(1.9) +Ag/Al_2O_3(0.8)[a]	3 : 100	20	94	0	6

[a] 1 : 1 (wt/wt) physical mixture.

Cu and Ag, separately supported on Al_2O_3 (Cu/Al_2O_3 and Ag/Al_2O_3), did not generate a comparable result to $CuAg/Al_2O_3$. In a previous paper,[19] we showed that pre-reduction in hydrogen at an optimized temperature is necessary for Cu/Al_2O_3 catalysts to generate good activity and selectivity. Interestingly, the activity of the Ag/Al_2O_3 catalyst is quite impressive considering the relatively low Ag loading. Its catalytic performance was better than those of the supported noble metal catalysts reported[7–13] in terms of activity and selectivity. This type of Ag/Al_2O_3 catalysts will be investigated further in a separate paper. The physical mixture of Cu/Al_2O_3(1.9) and Ag/Al_2O_3(0.8) generated a glycerol conversion of 20%, much higher than the sum of the conversions on Cu/Al_2O_3(1.9) and Ag/Al_2O_3(0.8) and comparable to that on $CuAg/Al_2O_3$(2.7)(7 : 3). It should be noted that the amount of alumina in the physical mixture doubles that in $CuAg/Al_2O_3$(2.7)(7 : 3). Although it has no activity in the absence of metals (as shown later in Fig. 6), alumina is not solely an inert support in the cases of alumina supported metal catalysts. It probably contributes to the glycerol conversion by promoting the formation of reaction intermediates on its acid sites, and also facilitating the hydrogen spillover discussed below.

It has been proposed[14,19,22] that coordinatively unsaturated copper species on the surface of Cu-based catalysts are the active sites for the hydrogenolysis of glycerol. That may be the reason that most of the Cu-based catalysts, such as Cu–ZnO, copper chromite, and Cu/Al_2O_3, usually need to undergo pre-reduction in order to possess activity. Cu–ZnO oxide catalysts showed some activity in the hydrogenolysis reaction without a high temperature pre-reduction,[14] but a high H_2 pressure (≥8 MPa) seems indispensable for the reaction. Under the reaction conditions employed here, however, we believe that such a reduction of CuO occurred significantly only when Ag co-existed on the catalysts presented in Table 2. For Al_2O_3 supported metal catalysts reported in the literature, spillover of activated hydrogen from Ag to MnO_2 and CoO[23] and from Pd to CuO[24] has been proposed to explain the reduction of the metal oxides. In our case, we believe that under the mild reaction conditions hydrogen was activated on the metallic Ag in the $CuAg/Al_2O_3$(2.7)(7 : 3) catalyst, and then spillover of hydrogen occurred to the CuO to reduce it *in situ* into Cu sites that are active for the reaction. This was confirmed by our TPR (Fig. 1) and XPS (Fig. 2) results.

The TPR pattern of Cu/Al_2O_3 displays a peak centered at about 250 °C, which corresponds to the reduction of the CuO starting at about 200 °C and finishing at about 260 °C. The pattern of the Ag/Al_2O_3 sample is similar to that of the Cu/Al_2O_3 catalyst except that the reduction of the silver oxide is in a much lower temperature region, from 50 to 120 °C. This

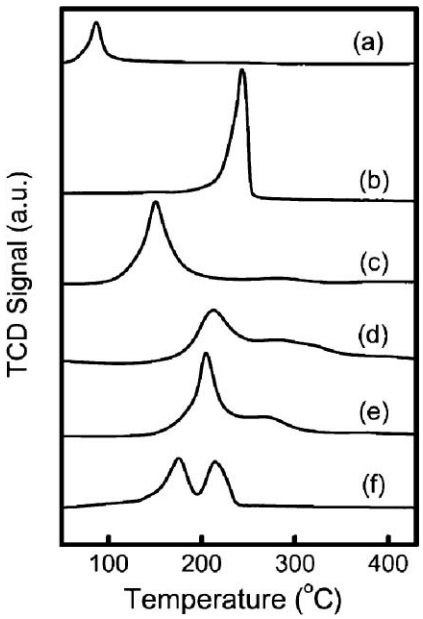

Fig. 1 TPR patterns of Cu and other metal impregnated Al_2O_3: (a) $Ag/Al_2O_3(2.0)$, (b) $Cu/Al_2O_3(2.0)$, (c) $CuAg/Al_2O_3(2.7)(7:3)$, (d) $CuZn/Al_2O_3(2.7)(7:3)$, (e) $CuCr/Al_2O_3(2.7)(7:3)$, and (f) $Cu/Al_2O_3(1.9)+Ag/Al_2O_3(0.8)$.

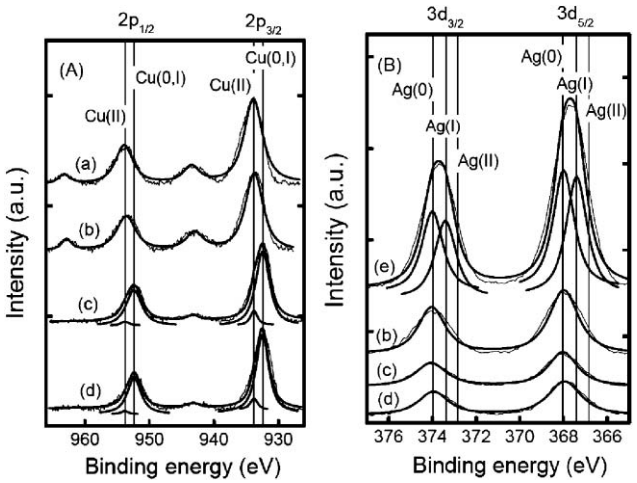

Fig. 2 XPS spectra in the binding energy range of (A) Cu 2p and (B) Ag 3d: (a) $Cu/Al_2O_3(1.9)$, (b) as-prepared $CuAg/Al_2O_3(2.7)(7:3)$, (c) $CuAg/Al_2O_3(2.7)(7:3)$ used at 200 °C, (d) $CuAg/Al_2O_3(2.7)(7:3)$ reduced in H_2 at 200 °C, and (e) $Ag/Al_2O_3(2.0)$.

means that any silver oxide on the Ag/Al_2O_3 catalyst can be reduced to metallic silver under our reaction conditions. The TPR pattern of the $CuAg/Al_2O_3$ catalyst contains a broad major peak around 150 °C, which could be assigned to the reduction of the CuO to metallic copper. The reduction of oxidic species on this catalyst is complete at about 200 °C. Therefore, we conclude that a similar reduction has happened under our reaction conditions (200 °C, 3.6 MPa H_2). It is clear that the Ag on the $CuAg/Al_2O_3$ catalyst lowered the reduction temperature of the copper oxide. Interestingly, the TPR pattern of the physical mixture of $Cu/Al_2O_3(1.9)$ and $Ag/Al_2O_3(0.8)$ showed two distinct CuO reduction peaks at around 175 and 215 °C. Apparently, the Ag species in the catalyst system promote the reduction of CuO, and this promotion is more effective when Ag and Cu are in close proximity. On the other hand, the TPR patterns of $CuZn/Al_2O_3(2.7)(7:3)$ and $CuCr/Al_2O_3(2.7)(7:3)$ showed major reduction peaks at about 210 °C and broad peaks above 250 °C. This means that the reduction of the CuO on these two Cu-based catalysts requires more severe conditions (temperature higher than 200 °C and/or higher H_2 pressure). The CuO on these catalysts was not (or not fully) reduced under our reaction conditions. In other words, Zn, Cr, Ni and Co are not as effective as Ag in terms of facilitating the reduction of CuO on the Al_2O_3 support. Other researchers indicated that the reduction temperature, needed to make Cu–ZnO[18] and copper chromite[25] active for the hydrogenolysis of glycerol, should be above 200 °C, and that these catalysts show poor activities when used without a reduction pre-treatment.

XPS spectra of as-prepared, used, and hydrogen reduced $CuAg/Al_2O_3$ catalysts are shown in Fig. 2. The XPS spectra of the Cu/Al_2O_3 and Ag/Al_2O_3 catalysts are presented for comparison. The analyses showed the oxidation states of those near-surface species. The spin–orbit split peaks at 952.5 eV ($2p_{1/2}$) and 932.3 eV ($2p_{3/2}$) (Fig. 2A) are attributed to Cu(0) and Cu(I).[26,27] Differentiation of these two oxidation states is not possible solely based on the 2p signals because the binding energy difference is only 0.1 eV.[26] Fully oxidized CuO species are characterized by both a second set of spin–orbit split peaks, shifted 1.3 ± 0.2 eV to higher binding energy (at 953.8 eV ($2p_{1/2}$) and 933.5 eV ($2p_{3/2}$)), and the appearance of characteristic satellite peaks around 963 and 943 eV.[26,27] XPS spectra in Fig. 2B displays the Ag 3d states of the catalysts. The spin–orbit split Ag peaks are around 374 eV ($3d_{3/2}$) and 368 eV ($3d_{5/2}$).[26,28,29] Compared with the metallic Ag peaks, the peaks of Ag species in the 1+ and 2+ (an average of 1+ and 3+) oxidation state are shifted to lower binding energies by 0.3 and 0.7 eV, respectively.[26] Sometimes ranges of binding energies, 368.0–368.3, 367.6–367.8, and 367.3–367.4 eV were reported for metallic Ag, Ag_2O, and AgO, respectively.[28]

Gaussian fitting of the Cu 2p binding energy region shows that the surface of $Cu/Al_2O_3(1.9)$ contains only CuO. The XPS spectrum of as-prepared $CuAg/Al_2O_3(2.7)(7:3)$ which was calcined at 400 °C in air also shows CuO as the only Cu species. After one reaction cycle at 200 °C in the presence of glycerol and hydrogen, the satellite peaks (963 and 943 eV) from the catalyst diminished significantly and the Cu 2p signals were slightly shifted to lower binding energy (952.5 and 932.3 eV), indicating that CuO was mostly reduced and that there was only a small amount of CuO left (7% based on deconvolution and peak area integration). The XPS spectrum of Cu species on $CuAg/Al_2O_3(2.7)(7:3)$ reduced at 200 °C with H_2 is almost identical to that of the used catalyst. This confirms that during reaction the bimetallic catalyst underwent an *in situ* reduction, which is very similar to that in H_2 at 200 °C.

The Ag 3d signals indicate that the Ag in the bimetallic catalysts is in the metallic state, while the $Ag/Al_2O_3(2.0)$ catalyst contains both Ag(0) and Ag(I). The amount of Ag(I) is about 50% of the total Ag in $Ag/Al_2O_3(2.0)$ (according to the XPS peak area). The observation of Ag(I) concurs with our TPR characterization (Fig. 1). The formation of metallic

Ag from the decomposition of Ag_2O or AgO in air has been investigated by Waterhouse *et al.* using XRD, FT-IR and Raman spectroscopies.[30] In the heating range of 100–200 °C, they observed the transformation of AgO (polycrystalline powder of silver(I,III) oxide) to Ag_2O, which was stable up to 350 °C and completely decomposed to Ag and O_2 at 400 °C. For Ag species on support, the states of Ag species may depend on the loading of the Ag and the nature of the support. Bethke and Kung[31] found that Ag/Al_2O_3 samples with 2 or 6 wt% Ag contained small Ag_2O particles and/or isolated Ag(I) atoms after calcination at 700 °C. Park and Boyer[32] claimed that Ag existed as well-dispersed Ag_2O on alumina support when the loading was 2 wt%, while metallic Ag appeared at 8 wt% Ag loading. This coincides with our observation of both metallic silver and silver oxide on $Ag/Al_2O_3(2.0)$. However, at present we do not have solid data to rationalize the absence of silver oxide on the $CuAg/Al_2O_3(2.7)(7:3)$ catalyst which contains about 7 wt% Ag. A hypothesis is that the Cu species in $CuAg/Al_2O_3(2.7)(7:3)$ facilitates the decomposition of Ag_2O by weakening the interaction between Ag_2O and the support or by consuming the oxygen in Ag_2O through formation of CuO.

Besides the ease of reduction, another contribution of Ag to the improved performance of the Cu-based supported catalyst could come from its capability to increase the dispersion of Cu species, which correlates with the amount of active Cu species available to the reactants. A comparison of the XRD patterns of $Cu/Al_2O_3(1.9)$ and $CuAg/Al_2O_3(2.7)(7:3)$ is made in Fig. 3. Although the $CuAg/Al_2O_3(2.7)(7:3)$ catalyst has the same Cu loading as the $Cu/Al_2O_3(1.9)$ catalyst, its XRD pattern does not display CuO peaks, as observed in the $Cu/Al_2O_3(1.9)$ catalyst. It seems that the addition of Ag helped the formation of well-dispersed Cu crystallites which were too small to be detected by the XRD analysis. Other metals (Zn, Cr) seem to be able to increase the Cu dispersion as well. No signals of Ag species were observed in the XRD spectrum of $CuAg/Al_2O_3(2.7)(7:3)$. Although the formation of Cu–Ag alloy cannot be completely ruled out, the chance should be slim considering the low calcination temperature and the oxidative environment.

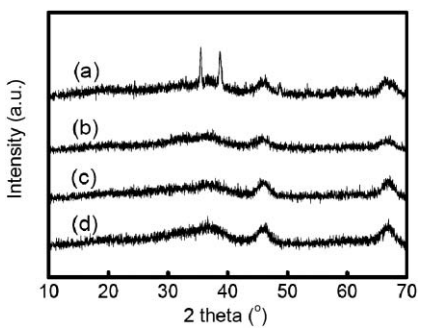

Fig. 3 XRD patterns of Cu and other metal impregnated Al_2O_3: (a) $Cu/Al_2O_3(1.9)$, (b) $CuAg/Al_2O_3(2.7)(7:3)$, (c) $CuZn/Al_2O_3(2.7)(7:3)$, and (d) $CuCr/Al_2O_3(2.7)(7:3)$.

Since the combination of Cu with Ag presented the best reaction results, the following studies were conducted on catalysts based on these two metals.

Effects of different supports. Strong effect of supports on the catalytic performance of supported CuAg bimetallic catalysts was observed for the hydrogenolysis of glycerol (Table 3). Among these supports, the Al_2O_3 stood out unambiguously. The more acidic supports, HZSM-5, HY, and Hβ, did not generate catalysts with high activity at the same loading of Cu and Ag. TPR characterizations presented in Fig. 4 show that the reduction of the metals on these supports was delayed to higher temperature when compared with the reduction on Al_2O_3. For example, the reduction of the HZSM-5 supported CuAg barely started until the temperature reached 250 °C and finished at about 400 °C. No glycerol conversion could be detected on $CuAg/HZSM-5(2.7)(7:3)$. We believe that a strong metal support interaction due to the strong acidity and high surface area of the supports (high metal dispersion) may hinder the reduction of copper oxide. It is known that transition metals on zeolites, when existing as framework metal cation[33] or metal silicate,[34] are hard to reduce due to their strong coordination to the oxygen atoms of the zeolite framework, especially on acidic zeolites.[33,35]

Table 3 Effects of different supports on catalytic performance

Catalyst	Conv. (%)	Selectivity (%)		
		1,2-PD	1,3-PD	Others
$CuAg/Al_2O_3(2.7)(7:3)$	27	96	0	4
$CuAg/HY(2.7)(7:3)$	2	80	2	18
$CuAg/H\beta(2.7)(7:3)$	2	89	1	10
$CuAg/HZSM-5(2.7)(7:3)$	nd[a]	—	—	—

[a] Not detected.

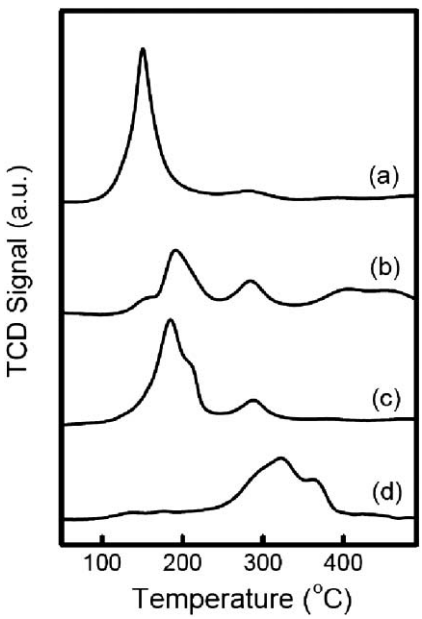

Fig. 4 TPR patterns of (a) $CuAg/Al_2O_3(2.7)(7:3)$, (b) $CuAg/HY(2.7)(7:3)$, (c) $CuAg/H\beta(2.7)(7:3)$, and (d) $CuAg/HZSM-5(2.7)(7:3)$.

The zeolites used in this study may also catalyze the dehydration of glycerol. Using FT-IR, Yada and Ootawa observed the selective formation of acrolein on H-MFI zeolite.[36] However, the large amount of water in our reaction system should limit the extent of acrolein formation. In addition, the

Table 4 Effect of Cu/Ag ratio of $CuAg/Al_2O_3$

Catalyst	Conv. (%)	Selectivity (%)		
		1,2-PD	1,3-PD	Others
$Cu/Al_2O_3(2.7)$	3	84	0	16
$CuAg/Al_2O_3(2.7)(95:5)$	21	99	0	1
$CuAg/Al_2O_3(2.7)(85:15)$	25	97	0	3
$CuAg/Al_2O_3(2.7)(70:30)$	27	96	0	4
$CuAg/Al_2O_3(2.7)(50:50)$	24	96	0	4
$CuAg/Al_2O_3(2.7)(30:70)$	25	95	0	5
$CuAg/Al_2O_3(2.7)(15:85)$	23	94	0	6
$CuAg/Al_2O_3(2.7)(5:95)$	23	93	0	7
$Ag/Al_2O_3(2.7)$	21	93	0	7

strong acidity of the zeolites may hinder the conversion of acrolein, as demonstrated by Volckmar *et al.* in their study of acrolein hydrogenation on silica/alumina supported silver catalysts.[37] Even if being hydrogenated, the product of acrolein hydrogenation would be propionaldehyde, allylalcohol or *n*-propanol rather than propanediols. All these factors contribute to the low conversion of glycerol and low propanediol selectivity on our zeolite-supported catalysts in Table 3.

Optimization of metal ratio and loading. $CuAg/Al_2O_3$ catalysts which have the same total metal loading (2.7 mmol of Cu and Ag) but various Cu to Ag molar ratios were prepared and tested (Table 4). In general, the bimetallic catalysts were more active than the monometallic ones. For example, $Cu/Al_2O_3(2.7)$ only presented a glycerol conversion of 3%. With replacement of 5% of the Cu by Ag, the glycerol conversion increased sharply to 21% on $CuAg/Al_2O_3(2.7)(95:5)$. With increased activities on these bimetallic supported catalysts, the selectivity to 1,2-PD increased to above 95% and little 1,3-PD was observed. The maximal conversion of about 27% was achieved on $CuAg/Al_2O_3(2.7)(70:30)$.

XRD patterns of $CuAg/Al_2O_3$ catalysts with various Cu to Ag ratios are presented in Fig. 5. The XRD pattern of $CuAg/Al_2O_3(2.7)(100:0)$, *i.e.* $Cu/Al_2O_3(2.7)$, clearly shows the existence of CuO crystallites on the catalyst surface. The signals of CuO were strongly attenuated once a small amount of Ag was added to the catalyst (Cu : Ag = 95 : 5). It is likely that CuO was well dispersed into small crystallites even at this low content of Ag. This supports the previous observation and confirms that the activity increase could partially come from good dispersion of CuO due to the Ag addition. Weak signals

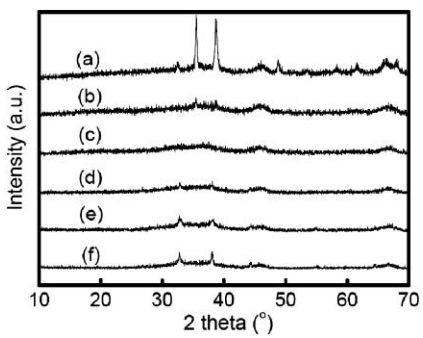

Fig. 5 XRD patterns of $CuAg/Al_2O_3(2.7)$ catalysts with various Cu/Ag molar ratios: (a) 100 : 0, (b) 95 : 5, (c) 70 : 30, (d) 30 : 70, (e) 5 : 95, and (f) 0 : 100.

of Ag_2O (2θ = 32.8, 38.2°) were observed in the XRD pattern of $CuAg/Al_2O_3(2.7)(0:100)$ (*i.e.* $Ag/Al_2O_3(2.7)$). In addition, XRD signals of metallic Ag (2θ = 38.2, 44.3°) besides Ag_2O was also detected on $Ag/Al_2O_3(2.7)$, consistent with the XPS observation in Fig. 2.

Reaction results on $CuAg/Al_2O_3$ catalysts with different total metal loadings (0.7 to 3.3 mmol g^{-1}) but a constant ratio of Cu/Ag (7 : 3) are displayed in Fig. 6. The glycerol conversion rose with increasing amount of supported active metals and reached a maximum (27%) at 2.7 mmol metals per gram of Al_2O_3, after which the conversion decreased with further increase of the metal loading. We believe that a serious pore blockage occurred at high metal loading, as indicated by the rapid loss of the surface area of the catalysts. The surface area of $CuAg/Al_2O_3(3.3)(7:3)$ was about 160 m^2 g^{-1} and of $CuAg/Al_2O_3(2.7)(7:3)$ it was about 200 m^2 g^{-1}. Therefore, the total amount of accessible active metal sites could have actually decreased although the total metal loading increased. The selectivity toward 1,2-PD (no 1,3-PD) was almost constant irrespective of the metal loading in the range studied.

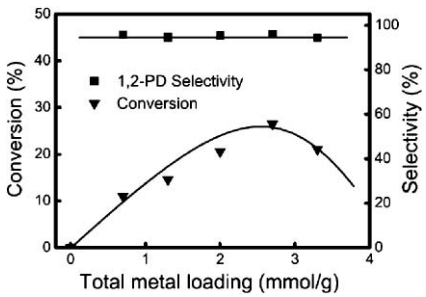

Fig. 6 Effect of total metal loading of $CuAg/Al_2O_3$ on the formation of propanediols from glycerol.

Through these studies, an optimized catalyst composition was established, *i.e.* 2.7 mmol of Cu and Ag (molar ratio 7 : 3) per gram of Al_2O_3 support.

3.2 Study of catalyst preparation procedure

Metal impregnation sequence. Since $CuAg/Al_2O_3(2.7)(7:3)$ consists of two catalytically active components, *i.e.* Cu and Ag, the effect of the metals impregnation sequence on the formation of propanediols from glycerol was investigated (Table 5). The catalyst prepared by simultaneously impregnating Cu and Ag salts onto the support showed the highest activity, about 7–9% higher than those on the other two catalysts prepared by loading the two metals sequentially, no matter which one was first.

TPR characterizations (Fig. 7) showed that all three catalysts have a maximal hydrogen consumption at about 150 °C. Besides this peak, the two catalysts prepared by sequential impregnations, especially $Cu/Ag/Al_2O_3(2.7)(7:3)$ in which Ag was impregnated first, also showed a broad peak centered around 190 °C, an indication that the promotion effect of Ag for the reduction of CuO on these two catalysts is not as effective as on the $CuAg/Al_2O_3(2.7)(7:3)$ catalyst. Instead of uniformly mixing well with Cu in the case of (c) simultaneous, Ag particles may sit on top of the CuO in the case of (a) Cu first, or be buried by the CuO in the case of (b) Ag first. Depending on the distance from the Ag, the CuO could be reduced at different

Table 5 Effect of Cu and Ag impregnation sequence

Catalyst	Impregnation sequence	Conv. (%)	Selectivity (%)			Surface ratio of Cu/Ag[b]
			1,2-PD	1,3-PD	Others	
$Ag/Cu/Al_2O_3(2.7)(7:3)$[a]	Cu first	20	93	0	7	52/48
$Cu/Ag/Al_2O_3(2.7)(7:3)$[a]	Ag first	18	93	0	7	51/49
$CuAg/Al_2O_3(2.7)(7:3)$	Simultaneous	27	96	0	4	65/35

[a] An extra calcination at 400 °C between the two sequential impregnations. [b] Based on XPS analysis.

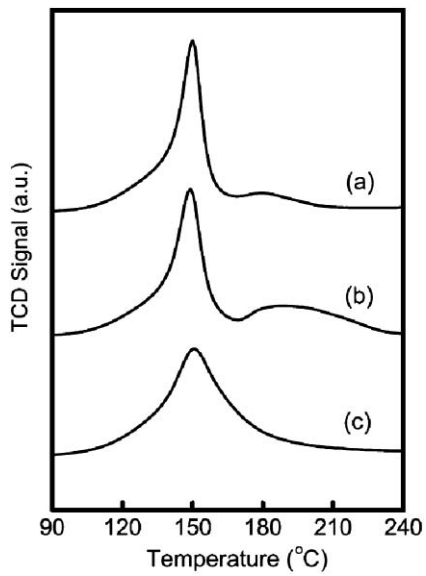

Fig. 7 TPR patterns of Cu and Ag impregnated Al_2O_3 with different impregnation sequences: (a) Cu first, (b) Ag first, and (c) simultaneous.

temperatures. The Cu close to the Ag would be reduced first and those relatively far away would have a delayed reduction. This could be why the TPR patterns of (a) and (b) in Fig. 7 showed two peaks. XRD signals of CuO were detected for the $Cu/Ag/Al_2O_3(2.7)(7:3)$ catalyst only (Fig. 8). This means that this catalyst has some CuO crystallites with relatively large sizes.

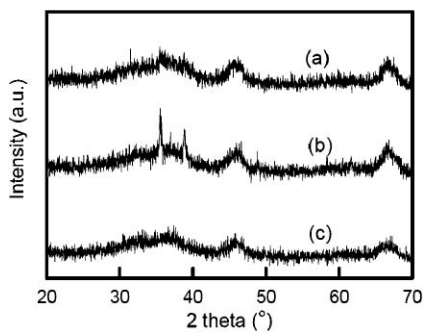

Fig. 8 XRD patterns of Cu and Ag impregnated Al_2O_3 with different impregnation sequences: (a) Cu first, (b) Ag first, and (c) simultaneous.

The relative amounts of Cu and Ag on the surfaces of the three catalysts were quantified with XPS analyses (Table 5). The surface Cu/Ag ratio on $CuAg/Al_2O_3(2.7)(7:3)$ was 65/35, slightly lower than the bulk ratio of Cu/Ag (7/3) in the catalyst. Considering that XPS is a semi-quantitative technique, we believe that both metals were almost homogeneously dispersed on this catalyst. On the two catalysts made by sequential impregnation, the Cu/Ag ratio is 52/48 for $Ag/Cu/Al_2O_3(2.7)(7:3)$ and 51/49 for $Cu/Ag/Al_2O_3(2.7)(7:3)$, much lower than for the simultaneously impregnated catalyst, which probably has the highest Cu dispersion.

It is believed that the low dispersion of the CuO and poor interaction between Cu and Ag resulted in the lower activities of the sequentially impregnated catalysts. To help the reduction and dispersion of the CuO, it seems vital for Ag and Cu to be mixed well in the impregnation solution and to contact the support at the same time so that they can be in a close vicinity.

Calcination temperature. The results in Fig. 9 illustrate a rise and fall in glycerol conversion when the calcination temperature rose from 200 to 500 °C. Maximal yield of 1,2-PD was achieved at 400 °C due to the highest glycerol conversion and the highest propanediol selectivity. Hence, calcining the catalyst at 400 °C for 3 h was the optimal treatment condition for this catalyst for the hydrogenolysis reaction.

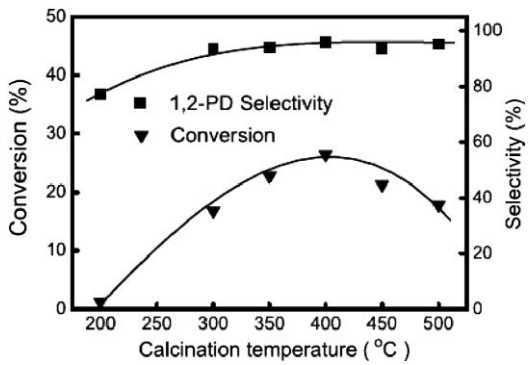

Fig. 9 Effect of calcination temperature of $CuAg/Al_2O_3(2.7)(7:3)$.

Fig. 10 shows the XRD patterns of $CuAg/Al_2O_3(2.7)(7:3)$ catalysts dried at 110 °C, calcined at 200, 400, and 500 °C. Weak signals assigned to $Cu(NO_3)_2$ crystallites ($2\theta = 13°$ and 26°) were observed on the sample dried at 110 °C and the one calcined at 200 °C. This means that the $Cu(NO_3)_2$ salt did not decompose completely at 200 °C or lower. No $AgNO_3$ crystallites ($2\theta = 24$, 32, 36 and 55°) were detected on these two samples, probably due to its high dispersion or easy decomposition at 200 °C or lower. The XRD patterns of the $CuAg/Al_2O_3(2.7)(7:3)$ catalysts calcined at 300, 400, and 500 °C, as well as their surface areas (about 200 $m^2\ g^{-1}$), were very similar. Neither the crystal phase of $Cu(NO_3)_2$ nor that of CuO was detected on these three samples. However, the samples calcined at 300 and 500 °C were only about 65% as active as the one calcined at 400 °C. These three catalysts were chosen for further studies with TPR and XPS.

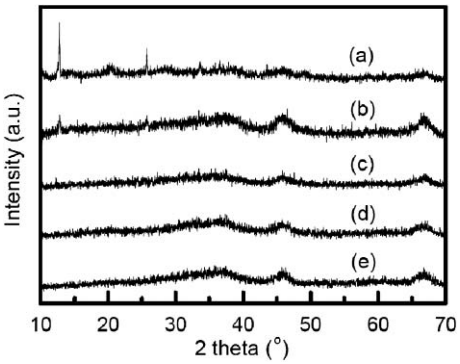

Fig. 10 XRD patterns of $CuAg/Al_2O_3(2.7)(7:3)$ calcined in air at (a) 110 °C, (b) 200 °C, (c) 300 °C, (d) 400 °C, and (e) 500 °C.

As shown by the TPR results in Fig. 11, the maximal hydrogen consumption on the 400 °C calcined sample appears at 150 °C. On the other two samples that had similar catalytic activities, the corresponding peaks are at about 160 °C. The order of the ease of reduction of these three catalysts was also confirmed by our XPS studies (Fig. 12). Before the spectra were taken, the three samples were pretreated in H_2 at 200 °C for 3 h to simulate the reducing environment during reaction. The XPS characterization revealed the difference of the relative amounts of low (0 or 1+) and high (2+) valence Cu species in the three catalysts (Fig. 12A). After the reduction, the majority of Cu species (93%) in the catalyst calcined at 400 °C is Cu(0) or Cu(I), while the ones calcined at 300 or 500 °C contain a much larger portion of Cu(II) (25–28%) besides Cu(0) and Cu(I).

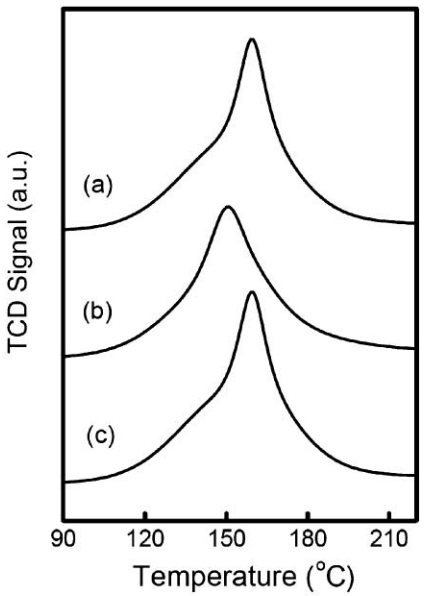

Fig. 11 TPR patterns of $CuAg/Al_2O_3(2.7)(7:3)$ calcined in air at (a) 300 °C, (b) 400 °C, and (c) 500 °C.

Using X-ray absorption near-edge structure and extended X-ray absorption fine structure, Wei and co-workers studied $Cu(NO_3)_2$ loaded aluminium oxide and showed that the prevailing Cu species (85%) on the sample calcined at 500 °C for 1 h was CuO, and that the remaining part of the Cu was present as $Cu(OH)_2$ (15%) and as a negligible amount of $Cu(NO_3)_2$.[38] Therefore, the $Cu(NO_3)_2$ on our 300 °C, 3 h calcined sample

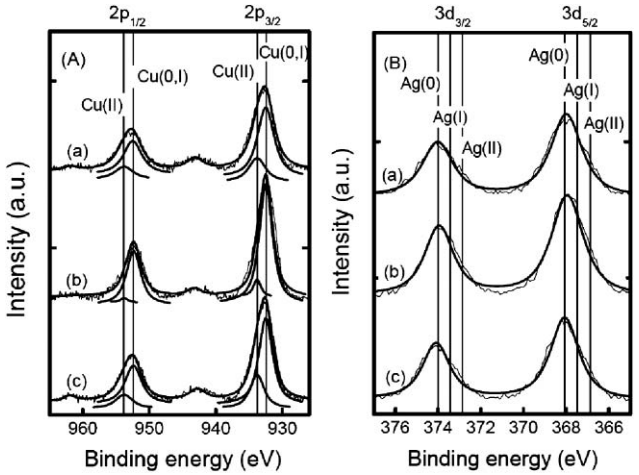

Fig. 12 XPS patterns in the binding energy range of (A) Cu 2p and (B) Ag 3d from $CuAg/Al_2O_3(2.7)(7:3)$ samples calcined in air at (a) 300 °C, (b) 400 °C, and (c) 500 °C, and then all reduced in H_2 at 200 °C.

should not have completely decomposed into CuO. This was confirmed by our study with thermal gravimetric analysis (result not shown here), which showed that most of the weight loss of the 110 °C pre-dried Cu/Al_2O_3 catalyst only occurred when the sample was heated in air at 10 °C min^{-1} to 400 °C. $Cu(OH)_2$ and/or $Cu(NO_3)_2$ from the incomplete decomposition may be more difficult to reduce than CuO. For the sample calcined at 500 °C, some copper aluminate may have been generated on the catalyst surface. Bolt *et al.*[39] studied the formation of nickel, cobalt, copper, and iron aluminates from α- and γ-alumina-supported oxides using Rutherford backscattering spectrometry, XRD, scanning electron microscopy, and UV-vis diffuse reflectance spectroscopy. They found that even at 500 °C small $CuAl_2O_4$ crystallites, which were invisible to XRD, were formed on the surface phase of each γ-alumina grain. Copper in the $CuAl_2O_4$ on Al_2O_3 is difficult to reduce. Plyasova *et al.*[40] showed that the reduction of bulk copper aluminate was significant only in the temperature range of 300 to 400 °C and did not reach 100% even at 700 °C. The Ag was present as metallic phase on all three samples after the H_2 treatment (Fig. 12B).

It is obvious that the calcination temperature has a strong influence on the interaction between Cu and Ag species and on the interaction between the metals and the support. For the binary oxide catalysts containing copper and silver, a proper calcination temperature might yield a suitable environment for easy hydrogen spillover from the Ag atoms to the Cu and/or a less electron drawing effect from the support as well so that the CuO could be easily reduced and stay in lower valences to act as catalytic active sites.

Comparison with a commercial catalyst. We tested a commercial copper chromite catalyst and compared its performance with our best bimetallic catalyst under the same reaction conditions (Fig. 13). The copper chromite, which with pre-reduction usually shows the best performance among Cu-based catalysts,[4,15] only had a glycerol conversion of 4% after 10 h when used directly after calcination in air (copper chromite (air)). Its activity increased to 13% after a reduction in H_2 at 300 °C (copper chromite (H_2)), but is still much lower than the one of $CuAg/Al_2O_3(2.7)(7:3)$, which was 27%. We

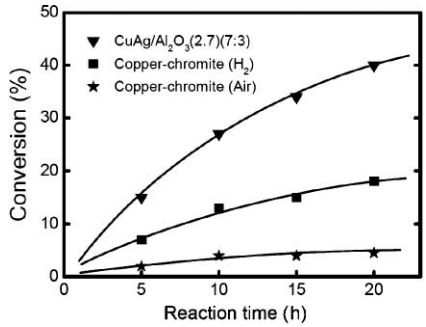

Fig. 13 Glycerol conversions on $CuAg/Al_2O_3(2.7)(7:3)$ and copper chromite at different reaction time.

attribute the low activity of the copper chromite mainly to its relatively low Cu dispersion. The propanediol selectivity of the copper chromite catalyst is about 80%, not as good as that of $CuAg/Al_2O_3(2.7)(7:3)$ either, which was above 95% consistently through out the reaction. The reaction rate on the $CuAg/Al_2O_3$ showed little change during the first 10 h but seemed to decrease gradually after that. Detailed study about deactivation is under way.

4. Conclusions

A γ-Al_2O_3 supported CuAg bimetallic catalyst can be used directly without a reduction pretreatment for glycerol hydrogenolysis to propanediols; it showed good performance under mild reaction conditions. The TPR and XPS characterizations revealed that the ease of the reduction of CuO on the supported bimetallic catalysts correlated well with the catalytic activity. The formation of low valence Cu species (Cu^0 or Cu^+) is the key for high activity. The addition of Ag to the Cu-based catalyst facilitated the reduction of the Cu species that generates low valence Cu species *in situ* under mild reaction conditions. XRD and XPS results showed that Ag could also improve the dispersion of the Cu species. The effects of Ag were not only dependent on the impregnation order of Cu and Ag, but also on the calcination temperature after the impregnation. When optimal amounts of Cu and Ag (Cu/Ag molar ratio 7 : 3, 2.7 mmol Cu+Ag per gram of γ-Al_2O_3) were loaded simultaneously on the support and calcined at 400 °C, a catalytic selectivity to propanediols of nearly 100% with a glycerol conversion of about 27% was achieved at 200 °C (1.5 MPa initial H_2 pressure, 10 h, M : G = 3 : 100) due to successfully suppressing the scission of the C–C bonds in glycerol, which often occurs on supported precious metal catalysts. Compared with a commonly used commercial copper chromite catalyst, the $CuAg/Al_2O_3$ catalyst had much higher activity and did not need a reduction pretreatment.

Acknowledgements

The authors thank the Educational Department of Liaoning Province, China for its financial support of this work (Grant# L2010036). The authors also thank the State Key Laboratory of Fine Chemicals at Dalian University of Technology for supporting the catalyst characterization work (Grant# KF0703). We would also like to acknowledge Prof. R. Prins (ETH) for helpful discussion.

References

1 R. D. Cortright, M. Sanchez-Castillo and J. A. Dumesic, *Appl. Catal., B*, 2002, **39**, 353–359.
2 G. Luo, S. Yan, M. Qiao, J. Zhuang and K. Fan, *Appl. Catal., A*, 2004, **275**, 95–102.
3 J. Chaminand, L. Djakovitch, P. Gallezot, P. Marion, C. Pinel and C. Rosier, *Green Chem.*, 2004, **6**, 359–361.
4 M. Pagliaro, R. Ciriminna, H. Kimura, M. Rossi and C. D. Pina, *Angew. Chem., Int. Ed.*, 2007, **46**, 4434–4440.
5 C. H. Zhou, J. N. Beltramini, Y. X. Fan and G. Q. Lu, *Chem. Soc. Rev.*, 2008, **37**, 527–549.
6 A. Behr, J. Eilting, K. Irawadi, J. Leschinski and F. Lindner, *Green Chem.*, 2008, **10**, 13–30.
7 I. Furikado, T. Miyazawa, S. Koso, A. Shimao, K. Kunimori and K. Tomishige, *Green Chem.*, 2007, **9**, 582–588.
8 J. Feng, H. Fu, J. Wang, R. Li and H. Chen, *Catal. Commun.*, 2008, **9**, 1458–1464.
9 T. Miyazawa, S. Koso, K. Kunimori and K. Tomishige, *Appl. Catal., A*, 2007, **318**, 244–251.
10 T. Miyazawa, S. Koso, K. Kunimori and K. Tomishige, *Appl. Catal., A*, 2007, **329**, 30–35.
11 M. Balaraju, V. Rekha, P. S. Sai Prasad, B. L. A. Prabhavathi Devi, R. B. N. Prasad and N. Lingaiah, *Appl. Catal., A*, 2009, **354**, 82–87.
12 A. Alhanash, E. F. Kozhevnikova and I. V. Kozhevnikov, *Catal. Lett.*, 2008, **120**, 307–311.
13 L. Ma, D. He and Z. Li, *Catal. Commun.*, 2008, **9**, 2489–2495.
14 S. Wang and H. C. Liu, *Catal. Lett.*, 2007, **117**, 62–67.
15 M. A. Dasari, P. P. Kiatsimkul, W. R. Sutterlin and G. J. Suppes, *Appl. Catal., A*, 2005, **281**, 225–231.
16 A. Perosa and P. Tundo, *Ind. Eng. Chem. Res.*, 2005, **44**, 8535–8537.
17 A. Yin, X. Guo, W. Dai and K. Fan, *Green Chem.*, 2009, **11**, 1514–1516.
18 M. Balaraju, V. Rekha, P. S. Sai Prasad, R. B. N. Prasad and N. Lingaiah, *Catal. Lett.*, 2008, **126**, 119–124.
19 L. Guo, J. Zhou, J. Mao, X. Guo and S. Zhang, *Appl. Catal., A*, 2009, **367**, 93–98.
20 R. T. Yang, *Adsorbents: Fundamentals and Applications*, Wiley, New York, 2003, p. 194.
21 J. Zhou, Y. Zhang, X. Guo, A. Zhang and X. Fei, *Ind. Eng. Chem. Res.*, 2006, **45**, 6236–6242.
22 D. G. Lahr and B. H. Shanks, *J. Catal.*, 2005, **232**, 386–394.
23 M. Luo, X. Yuan and X. Zheng, *Appl. Catal., A*, 1998, **175**, 121–129.
24 T. Inui, H. Hara, T. Takeguchi and J. Kim, *Catal. Today*, 1997, **36**, 25–32.
25 X. Huang, L. Ma and M. S. Wainwright, *Appl. Catal., A*, 2004, **257**, 235–243.
26 R. Morrish and A. J. Muscat, *Chem. Mater.*, 2009, **21**, 3865–3870.
27 J. Batista, A. Pintar, D. Mandrino, M. Jenko and V. Martin, *Appl. Catal., A*, 2001, **206**, 113–124.
28 F. Xiao, H. Liu and Y. Lee, *Bull. Korean Chem. Soc.*, 2008, **29**(12), 2368–2372.
29 J. F. Weaver and G. B. J. Hoflund, *J. Phys. Chem.*, 1994, **98**, 8519–8524.
30 G. I. N. Waterhouse, G. A. Bowmaker and J. B. Metson, *Phys. Chem. Chem. Phys.*, 2001, **3**, 3838–3845.
31 K. A. Bethke and H. H. Kung, *J. Catal.*, 1997, **172**, 93–102.
32 P. W. Park and C. L. Boyer, *Appl. Catal., B*, 2005, **59**, 27–34.
33 R. Bulánek, B. Wichterlová, Z. Sobal'ık and J. Tichý, *Appl. Catal., B*, 2001, **31**, 13–25.
34 S. Jong and S. Cheng, *Appl. Catal., A*, 1995, **126**, 51–66.
35 A. Jones and B. D. McNicol, Temperature Programmed Reduction for Solid Materials Characterization, in *Chemical Industries*, Vol. 24, Marcel Dekker, New York, 1986, p. 30.
36 E. Yoda and A. Ootawa, *Appl. Catal., A*, 2009, **360**, 66–70.
37 C. E. Volckmar, M. Brona, U. Bentrup, A. Martin and P. Claus, *J. Catal.*, 2009, **261**, 1–8.
38 Y. Wei, H. Wang, Y. Yang and J. Lee, *J. Phys.: Condens. Matter*, 2004, **16**, S3485–S3490.
39 P. H. Bolt, F. H. P. M. Habraken and J. W. Geus, *J. Solid State Chem.*, 1998, **135**, 59–69.
40 L. M. Plyasova, T. M. Yur'eva, I. Y. Molina, T. A. Kriger, A. M. Balagurov, L. P. Davydova, V. I. Zaikovskii, G. N. Kustova, V. V. Malakhov and L. S. Dovlitova, *Kinet. Catal.*, 2000, **41**, 429–436.